Kinetic Studies of Lignin Solvolysis and Reduction by Reductive Catalytic Fractionation Decoupled in Flow-Through Reactors

ACS Sustainable Chemistry & Engineering

Research Article

Cite This: ACS Sustainable Chem. Eng. 2018, 6, 7951−7959

pubs.acs.org/journal/ascecg

Kinetic Studies of Lignin Solvolysis and Reduction by Reductive Catalytic Fractionation Decoupled in Flow-Through Reactors

Eric M. Anderson,[†] Michael L. Stone,[†] Max J. Hülsey,[†] Gregg T. Beckham,*[,‡] and Yuriy Román-Leshkov*[,†]

[†]Chemical Engineering, Massachusetts Institute of Technology, 25 Ames Street, Cambridge, Massachusetts 02139, United States

[‡]National Renewable Energy Laboratory, 15013 Denver West Parkway, Golden, Colorado 80401, United States

Supporting Information

ABSTRACT: Reductive catalytic fractionation (RCF) is an effective active-stabilization strategy to selectively extract and depolymerize lignin into aromatic monomers. Here, the kinetics of RCF were investigated by using flow-through reactors to decouple the two limiting mechanistic steps, namely lignin solvolysis and reduction. When operating in a solvolysis-limited regime, apparent energy barriers of 63 ± 1 and 64 ± 2 kJ mol^{-1} were measured for the solvent mediated lignin extraction of poplar using particle diameters of 0.5 < d < 1 mm and 0.075 < d < 0.25 mm, respectively. In contrast, when using mechanically stirred batch reactors, apparent barriers of 32 ± 1 and 39 ± 3 kJ mol^{-1} were measured for particle diameters of 0.5 < d < 1 mm and 0.075 < d < 0.25 mm, respectively. The difference of activation barriers between flow and batch reactors indicated that lignin extraction under typical RCF conditions in a 100 mL batch reactor stirred at 700 rpm was mass-transfer limited. In the reduction-limited regime, cleavage of the β-O-4 bond in a model compound exhibited an apparent activation barrier of 168 ± 14 kJ mol^{-1}. This study demonstrates RCF occurs by two limiting processes that can be independently controlled. Furthermore, both controlling which process limits RCF and verifying if transport limitations exist, are critical steps to develop a mechanistic understanding of RCF and to design improved catalysts.

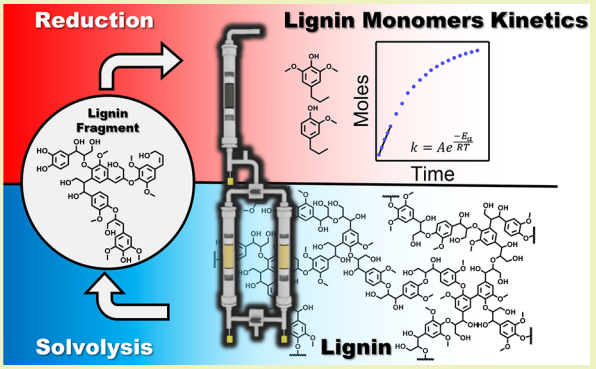

KEYWORDS: *Lignin conversion, Biomass pretreatment, Flow-through extraction, Lignin kinetics, Reductive catalysis, Lignin first, Semicontinuous processing*

INTRODUCTION

Lignin, an oxygen rich aromatic polymer that accounts for 15−30% of biomass, is a sustainable and renewable source of aromatic carbon. Many pretreatment techniques have been developed over the past decades to remove lignin from biomass. Thermochemical pretreatments have proven effective at removing or redistributing lignin but result in the conversion of C−O ether bonds in the lignin structure into a network of C−C bonds.[1,2] The formation of this recalcitrant network makes the selective conversion of lignin into aromatic chemicals difficult, ultimately leading to lignin incineration as a low-grade fuel.[3] Consequently, extraction techniques that facilitate the selective conversion of lignin into valuable chemicals and high grade fuels could add significant value to the biorefining process.[4−7]

Recently, a variety of active stabilization methods have been developed to simultaneously extract and depolymerize lignin into a narrow slate of aromatic monomers and small oligomers while preserving the carbohydrate fraction for downstream processing.[8−10] One particularly promising technique is reductive catalytic fractionation (RCF), which uses a reduction catalyst to quench reactive intermediates produced from lignin solvolysis[11−19] and prevent undesirable C−C coupling reactions. This method generates a narrow slate of oxygenated arenes from lignin, while mostly preserving both the hemicellulose and cellulose fractions of biomass as a solid residue.[20] RCF is typically performed in batch reactors where untreated biomass particles are mixed with a redox-active catalyst, such as supported Pd,[21] Ru,[22] or Ni, in a polar protic solvent containing a hydrogen donor such as hydrogen gas (pressures ranging from 30 to 60 bar) or isopropyl alcohol,[15] and in some cases a cocatalyst, such as a Brønsted[12,19,23] or Lewis acid,[24−26] at temperatures ranging from 180 to 250 °C.[27] RCF is hypothesized to occur by two independent consecutive steps, namely lignin solvolysis followed by reduction (illustrated in Figure 1).[14,23,28−30] Lignin solvolysis is the solvent-facilitated extraction of lignin from the plant cell walls that generates a mixture of soluble oxoaromatic fragments. These fragments then migrate to the surface of the redox-active catalyst to

Received: March 20, 2018
Published: April 24, 2018

DOI: 10.1021/acssuschemeng.8b01256
ACS Sustainable Chem. Eng. 2018, 6, 7951−7959

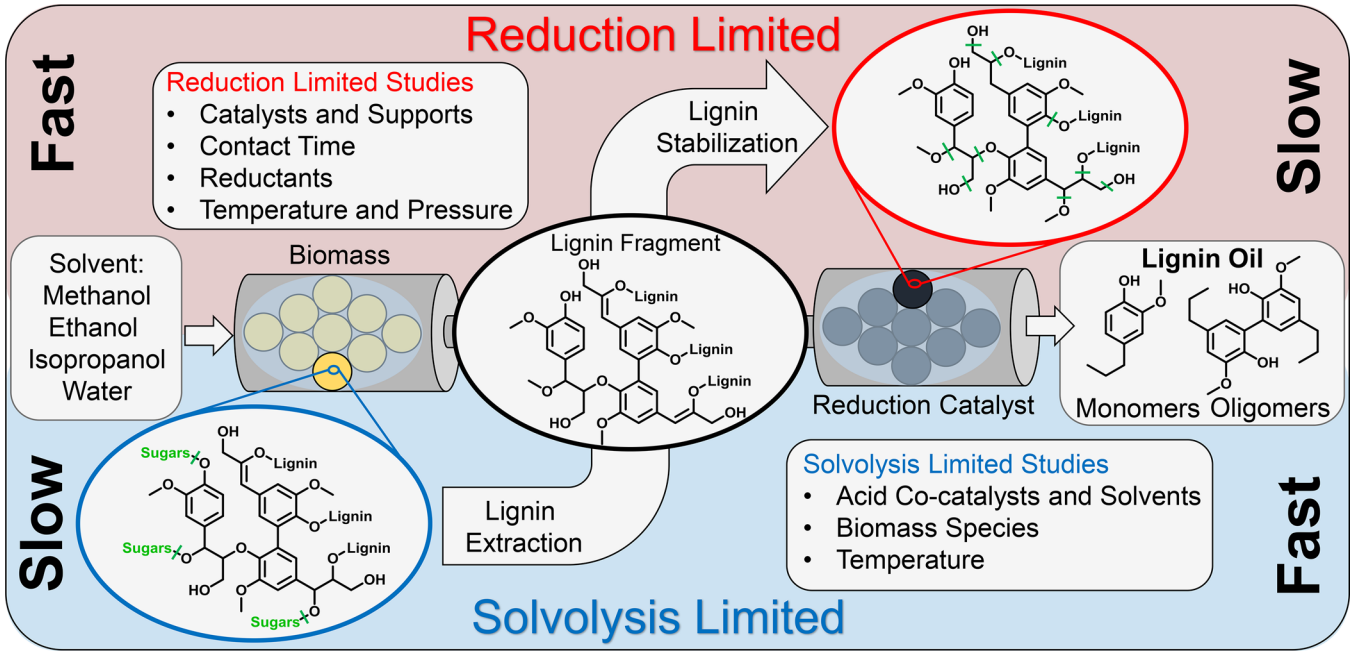

Figure 1. Schematic illustrating the RCF limiting regimes of lignin solvolysis and reduction, which can be physically separated and isolated by manipulating the rates of the two independent steps in flow-through reactors. A solvolysis limited regime exists when solvolysis is slow compared to reduction (blue), while a reduction-limited regime exists when reduction is slow compared to solvolysis (red). Operating in each of these regimes allows performing focused studies about specific RCF process parameters. Green lines signify bonds broken in each step.

undergo reduction. Specifically, the aryl ether bonds (primarily β-O-4, with 4-O-5 and α-O-4 as minor components) are cleaved by hydrogenolysis, while reactive C−C double bonds are either partially or fully hydrogenated to create stable monomers and oligomers. The resulting stabilized mixture containing oxygenated aromatic monomers and oligomers is recovered as a lignin oil. Although many studies on RCF have been reported in the literature, key questions still remain unresolved, particularly with respect to our collective understanding of the operating regimes for each of its independent steps. This information is critical to gain fundamental insights into the dynamics of lignin detachment from biomass, the development of new and improved reduction catalysts, and the optimization and scale up of RCF into a viable biomass fractionation strategy.

The total lignin oil (i.e., monomers + oligomers) recovered after reaction, the relative number of monomers within the lignin oil, and the degree of side chain saturation (i.e., propyl vs propenyl) in the monomer population represent three important metrics that can be used to understand RCF. At the limit of full lignin extraction and conversion, the total amount of lignin oil produced will depend on the initial lignin content in the original biomass; the relative ratio of monomers to lignin oil will depend on the biomass type and the intrinsic amount of cleavable β-O-4, 4-O-5, and α-O-4 bonds; and the degree of side saturation will depend on the activity and stability of the catalyst. Indeed, tracking these three metrics as a function of time under different reaction conditions can enable identification and analysis of the limiting regimes for both lignin solvolysis and reduction.

As illustrated in Figure 1, operating either at the limiting conditions for solvolysis (i.e., when lignin fragment detachment is slow relative to the time scale of the total number of turnovers for reductive bond cleavage at the catalyst surface) or at those for reduction (i.e., when lignin solvolysis is fast relative to the time scale of reductive bond cleavage of lignin fragments) enables interrogating and optimizing different aspects of the RCF process. For example, a solvolysis limiting condition is required to investigate the influence of a solvent additive (e.g., an acid) on lignin solubilization from the cell wall. Otherwise, if the system were operated in a reduction-limited regime, there would be no observable changes in monomer yields even if the additive were to accelerate solvolysis rates. Similarly, a reduction-limited regime is required to study catalyst activity and stability profiles by tracking monomer yields and degree of side-chain unsaturation. Otherwise, an identical monomer yield and degree of saturation would be obtained when operating in a solvolysis-limited regime since the fast reduction time scale would convert all of the lignin intermediates before any differences could be observed. Equally important is having the capability of identifying reaction conditions in which heat and mass transfer limitations may influence the apparent reaction kinetics in each regime. Unfortunately, based on their intrinsic operation, batch reactors are not suitable to easily identify, isolate, and study these limiting conditions. To this end, the concept of flow-through reactors for RCF that are capable of physically separating and decoupling the solvolysis and reduction steps was recently demonstrated by Roman-Leshkov et. al. and Samec et. al.[31,32]

In the present work, flow-through reactors operated at different reaction conditions were used to isolate the lignin solvolysis and reduction steps and measure their intrinsic kinetic parameters. Lignin solvolysis was investigated using untreated poplar wood, while the reduction kinetics were studied with a model β-O-4 compound, 1-(3,4-dimethoxyphenyl)-2-(2-methoxyphenoxy)propane-1,3-diol (hereafter denoted as POPV).[33] These data were compared to data obtained in traditional batch systems, revealing strong mass-transfer limited conditions for batch reactor systems operated at

DOI: 10.1021/acssuschemeng.8b01256
ACS Sustainable Chem. Eng. 2018, 6, 7951−7959

analogous temperature and pressures. Overall, we demonstrate that flow-through reactors provide important advantages to understand the mechanistic underpinnings of the RCF process.

EXPERIMENTAL SECTION

Catalyst Synthesis. Nickel on carbon (Ni/C) catalysts with different nickel loadings were synthesized by a wet impregnation method. A desired amount of nickel nitrate hexahydrate (Sigma-aldrich) was dissolved in deionized water and added to Darco carbon (Sigma-aldrich, 100 mesh) at a water to carbon ratio of 0.8 g/g to form 10 g of total catalyst. The mixture was allowed to equilibrate for 16 h and then dried at 120 °C for 24 h. The catalyst was then reduced in a tube furnace. The catalyst was heated to 450 °C over 1 h and then held for 2 h at 450 °C under flowing nitrogen (100 mL min^{-1}). The catalyst was used without further treatment in batch reactions. Catalysts used in flow reactions were made by creating a physical mixture of 50/50 w/w Ni/C and SiO_2 (Sigma-aldrich, 12 nm). The solid mixture was agitated for 24 h with a magnetic stir bar. The resulting physical mixture was pelletized to 100−200 mesh.

Compositional Analysis of Biomass. Compositional analysis of poplar was performed by the standard NREL Laboratory Analytical Procedure (LAP).[34,35] First, high pressure and temperature extractions were performed on the biomass to remove extractives. The poplar (0.3 g) was then subjected to 72 wt % sulfuric acid (3 mL) for 1 h at 30 °C to dissolve both cellulose and hemicellulose. The concentrated slurry was then diluted to 4 wt % with water. The slurry was heated in an autoclave at 121 °C for 1 h. The slurry was filtered to yield an acid insoluble lignin rich fraction. The ash content was determined by oxidizing the acid insoluble lignin fraction at 575 °C for 24 h in air. The remaining acid soluble lignin was determined by UV/vis spectroscopy (Thermo Scientific Nanodrop 8000 spectrophotometer), using absorbance measurements at 320 nm with an extinction coefficient of 2.5. The sugar content was determined by high performance liquid chromatography (HPLC, Agilent 1100 HPLC) using a refractive index detector (RI) at 85 °C. A Shodex Sugar SP0810 column equipped with a guard column was used for analysis at 85 °C with a flow rate of 0.6 mL min^{-1} of HPLC grade water as the mobile phase.

Model β-O-4 Compound Synthesis. The synthesis of the model β-O-4 was previously reported.[33] All chemicals and reagents were purchased from Sigma-aldrich and used as purchased. First, methyl 2-bromoacetate (10.22 g, 1.3 equiv) was coupled to guaiacol (6.25 g, 1 equiv) by refluxing in acetone (80 mL) and potassium carbonate (20.83 g, 3 equiv) for 3 h producing methyl-2-(2-methoxyphenoxy)-acetate. Acetone was removed under vacuum to produce an oil which was crystallized out of methanol (S, 7.54 g, 77% yield). ^{1}H NMR ($CDCl_3$, 400 MHz) δ = 3.79 (s, 3H), 3.88 (s, 3H), 4.70 (s, 2H), 6.85−6.99 ppm (m, 4H).

Methyl-2-(2-methoxyphenoxy)acetate was added to 3,4-dimethoxybenzaldehyde by an aldol condensation. Dry THF (30 mL) and 1 M LDA solution (40 mL) were cooled down to −78 °C in a Schlenk flask under nitrogen gas. Methyl-2-(2-methoxyphenoxy)acetate (7.39 g, 1 equiv) dissolved in dry THF (40 mL) was added slowly through a septum. After stirring the mixture for 15 min, a solution of the 3,4-dimethoxybenzaldehyde (6.34 g, 1.02 equiv) in dry THF (40 mL) was added dropwise. The mixture was stirred at −78 °C for 2 h and at RT for 30 min. The reaction mixture was cooled down to −78 °C again and a solution of NH_4Cl in DI water was added slowly. The mixture was then extracted 4 times with 40 mL ethyl acetate each. Combined organics were washed with brine once, dried and removed under vacuum. Flash column chromatography (SiO_2; 58% hexanes, 42% acetone, $R_f \sim 0.25$) was done to give methyl 3-(3,4-dimethoxyphenyl)-3-hydroxy-2-(2-methoxyphenoxy) propanoate (S, 3.68 g, 27% yield). ^{1}H NMR ($CDCl_3$, 400 MHz) δ = 3.53−3.55 (dd, 1H), 3.60 (s, 3H), 3.77 (s, 3H), 3.78 (s, 6H), 4.64−4.65 (d, 1H), 5.02−5.05 (d, 1H), 6.75−6.99 ppm (m, 7H)

1-(3,4-Dimethoxyphenyl)-2-(2-methoxyphenoxy)propane-1,3-diol was produced by reducing the ester of 3-(3,4-dimethoxyphenyl)-3-hydroxy-2-(2-methoxyphenoxy)propanoate with sodium borohydride. A Schlenk flask was charged with methyl 3-(3,4-dimethoxyphenyl)-3-hydroxy-2-(2-methoxyphenoxy) propanoate (3.48 g, 1 equiv) and purged with nitrogen. THF/water (3:1, 80 mL) mixture was added through a septum. Sodium borohydride (1.90 g, 5.2 equiv) was added in three portions over 1 h under nitrogen flow. The mixture was then stirred for 18 h. The solvents were removed under vacuum until ∼20 mL were left. DI water (100 mL) was added and the mixture was extracted with ethyl acetate (4 × 50 mL). Combined organics were dried over sodium sulfate and removed under vacuum. Flash column chromatography (SiO_2; 53% acetone, 47% hexanes, $R_f \sim 0.25$) was done to give 1-(3,4-dimethoxyphenyl)-2-(2-methoxyphenoxy)-propane-1,3-diol (oil, 2.60 g, 81%). ^{1}H NMR ($CDCl_3$, 400 MHz) δ = 3.64−3.94 (m, 13H), 4.14−4.18 (m, 1H), 4.98−4.99 (d, 1H), 6.82−7.08 ppm (m, 7H). ^{13}C NMR ($CDCl_3$, 100 MHz) δ = 55.85, 55.89, 55.90, 60.80, 72.72, 87.02, 109.32, 110.98, 112.16, 118.51, 120.57, 121.58, 123.99, 132.74, 146.93, 148.41, 148.95, 151.40 ppm.

Biomass Reactivity Studies. Batch reactions were performed using a mechanically stirred batch reactor (Parr Instruments, 4560 series, 100 mL) equipped with an overhead stirrer. Poplar (26 wt % lignin, supplied by Idaho National Laboratory, Morrow, Oregon) used for batch experiments was milled and sieved to either 0.5 < d < 1 mm or 0.075 < d < 0.25 mm. Milled poplar (1 g), catalyst (0.15 or 0.20 g), and methanol (50 mL) were charged to the reactor. The reactor was pressurized to either 1.5 or 3 MPa with hydrogen gas and heated to 200 °C over 0.5 h at 700 rpm. After the desired batch reaction time was reached, the reaction was quenched by rapid cooling in an ice bath. The reaction slurry was then filtered with a 0.2 μm filter. The methanol was then removed under vacuum and the resulting oil was dissolved in dichloromethane (DCM)/water (1:1 v/v, 20 mL). The extraction was performed to remove water-soluble sugars from the organic soluble lignin derived products. The water was extracted with additional dichloromethane (2 × 10 mL). The dichloromethane was removed under vacuum affording lignin oil. The lignin products were quantified from this oil.

Model compound flow reactions were performed in a gas−liquid phase, packed-bed reactor. The reactor was constructed of 0.25 in (OD) stainless steel tubing. The catalyst bed in each reactor was made from a physical mixture of 50/50 w/w 5% Ni/C and SiO_2. The catalyst was pelletized to a mesh size of 100−200 mesh and mixed with SiC (120 mesh, Alfa Aesar) to form the catalyst bed. The bed was held in place by two glass wool plugs located above and below the bed. The rest of the reactor void volume was filled with 1 mm glass beads. The reaction temperature was measured directly below the catalyst bed with a K-type thermocouple (Omega). The tubular reactor was heated in a furnace (Applied Test Systems 3210) with an aluminum sleeve to enhance heat transfer and the temperature was controlled with a Digi sense temperature controller (TC9500). The liquid with reactant dissolved (2 or 4 mg mL^{-1}) was delivered to the inlet of the reactor by an HPLC pump (waters 515). Hydrogen gas was mixed with the liquid upstream of the reactor and controlled with a mass flow controller (Brooks SLA5850S). The effluent of the reactor was sent to a high pressure, gas−liquid settler (Gage & Valve Co.) where the gas was vented through a back-pressure regulator (Swagelok 0−1000 psig KPB1L0A412P20000) to maintain the reaction pressure (60 bar), and the liquid was accumulated in the separator. Liquid samples were taken from the separator to quantify products produced from the reaction by GC-FID (Agilent, details below).

Flow-through RCF was performed in a flow-through dual bed reactor (FDBR) which was constructed by adding an additional upstream reactor to the reactor used for model compounds (Figure S1). The upstream attachment contained two stainless steel reactors (0.5 in OD) which were heated with heat tape (Briskheat TBIH051-040LD) and controlled with a Digi sense temperature controller (TC9500). The reactors were filled with 1 g of poplar wood held in place with two glass wool plugs above and below the bed. The rest of the void volume was filled with 1 mm glass beads. A K-type thermocouple (Omega) was placed directly below the bed for temperature control. The solvolysis reactors were setup in parallel such that the flow of solvent into the bed could be diverted from a spent biomass bed to a fresh biomass bed loaded in an adjacent

DOI: 10.1021/acssuschemeng.8b01256
ACS Sustainable Chem. Eng. 2018, 6, 7951−7959

reactor. The outlet of either biomass reactor fed directly to a 0.25 in (OD) reactor containing 0.3 g 15% Ni/C (50/50 SiO_2, 100–200 mesh) packed in an identical fashion to the model compounds studies. Reaction samples were taken every 10 min from the gas liquid separator and analyzed by gas chromatography-flame ionization detector (GC-FID). Liquid oil yields were determined from binned samples which were extracted with DCM/water (3 × 10 mL).

Lignin Monomer Quantification. Samples were quantified using an Agilent 7890A GC. A 1 μL injection was used with a split ratio of 10:1 and a 30 m × 250 μm × 0.25 μm Agilent Technologies DB-1701 column. The inlet temperature was set to 280 °C, and the oven was programmed to ramp from 50 to 280 °C at a rate of 10 °C min^{-1} for a total run time of 29 min. An FID was used to quantify the products. Samples were prepared with dimethoxybenzene as an external standard.

RESULTS AND DISCUSSION

Isolation of limiting RCF operating regimes by changing conditions in batch reactions. The solvolysis- and reduction-limited regimes of RCF were first isolated using batch reactors by changing catalyst loading and hydrogen pressure. Although the rates of both processes can be controlled independently given that the catalyst is only required for the reduction step, it is difficult to measure the two rates separately because the products of lignin solvolysis (and thus reactants in lignin reduction) are oligomers of varying chemical composition. The identification and quantification of every oligomeric species present after reaction is a major analytical undertaking and was outside the scope of this study. As a proxy, the production rate of total lignin oil (i.e, monomers + oligomers)—a measure of total lignin extraction—was used to track the extent of solvolysis, and the rate of monomer production from the extracted lignin oil was used to track the reduction step. Lignin solvolysis rates only depend on the solvent type and solvolysis temperature, resulting in identical solvolysis rates (as measured by total lignin oil recovered) when varying the catalyst loading and hydrogen pressures. However, for a given solvolysis rate, the catalyst loading and hydrogen pressure can alter the reduction rate, thus impacting monomer generation when the reactor operates in a regime below the maximum monomer yield (i.e., <100% conversion of oligomers to monomers via reduction). Figure 2 shows the two limiting regimes obtained in batch systems sampled at 1 h (thus representing a single time point in the conversion profile) and operated at 200 °C using different catalyst loadings. The solvolysis-limited regime is depicted in the right side of Figure 2 using a total hydrogen pressure of 30 bar. Using a catalyst loading of 5 wt % Ni/C, a monomer yield of 17.3 wt % was obtained with a propenyl side chain hydrogenation selectivity of 66%. When the catalyst loading was increased to 10 wt % Ni, the monomer yield increased to 19.7 wt % with 89% hydrogenation selectivity. Increasing the catalyst loading to 15% produced 19.4 wt % monomers with 92% hydrogenation selectivity. A constant monomer yield invariant to catalyst loading indicated that the lignin monomer yield was limited by solvolysis; because lignin detachment was slow relative to the time scale of total turnovers of the catalyst. Conversely, batch reactions at 15 bar of hydrogen resulted in a monotonically increasing monomer yield from 11.0 to 19.5 wt % when the catalyst loading was increased from 5 to 15 wt % Ni/C. The degree of propenyl side chain hydrogenation selectivity also increased from 15% to 58% as the catalyst loading increased. Additionally, the total lignin oil yield was nearly constant for the three different batch reactions indicating that the solvolytic

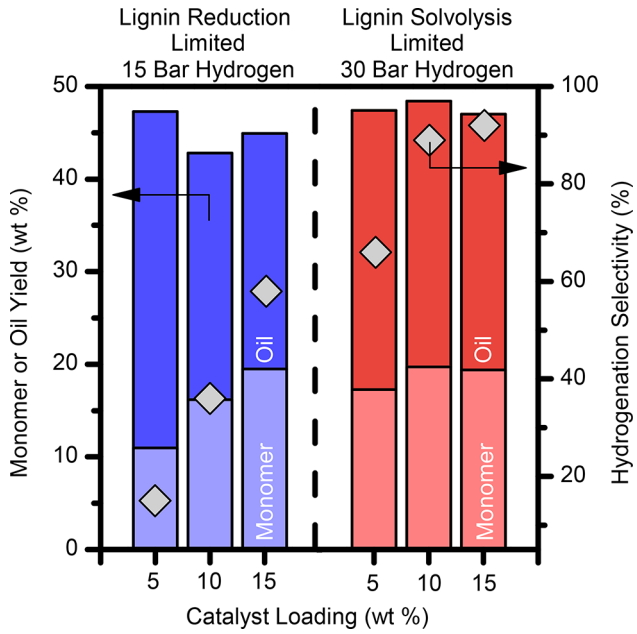

Figure 2. Lignin solvolysis and reduction limiting conditions achieved by changing hydrogen pressure and the weight loading of Ni on carbon in batch reactors. The bars indicate monomer and oil yields while the gray diamonds reference the side chain hydrogenation selectivity for each reaction. Reaction conditions: 1 g poplar (26% lignin), 0.2 g catalyst, 50 mL MeOH, 1 h reaction (0.5 h heat up), 15 or 30 bar H_2, 200 °C and 700 rpm.

extraction of lignin was fast and not dependent on the catalyst loading. Taken together, the constant lignin oil with increasing monomer yields that were proportional to catalyst loading revealed conditions limited by reduction. The existence of these limiting regimes means that, by choosing the appropriate conditions, it is possible to decouple the RCF process and study the kinetics of each process independently.

Determination of Solvolysis Limited Activation Barriers in Flow-Through and Batch Reactors. Lignin solvolysis activation barriers were measured in the FDBR using the initial rates generated from both monomer and lignin oil yields. Under solvolysis-limiting conditions, when complete conversion of all lignin fragments is achieved in the reduction step, these two activation barriers should be identical. Therefore, this measurement serves as a useful method to verify solvolysis limiting conditions experimentally. The initial solvolysis rate based on monomer generation was found by fitting the cumulative monomer yields from products sampled every 10 min over a 1 h extraction period (Figure S2).[31] The initial solvolysis rate based on lignin oil yields was determined from the total amount of lignin oil accumulated over the 1 h extraction times. Reactions were performed using 1 g of poplar ($0.5 < d < 1$ mm) and 0.3 g of 15% Ni/C (50/50 SiO_2, 100–200 mesh), operating at 60 bar of H_2 gas (50 mL min^{-1} H_2 STP) with a MeOH flow rate of 0.5 mL min^{-1} (the Reynolds number for these conditions is 0.3, implying laminar flow in the packed bed reactor, eq S1).[36] The catalyst bed was maintained at 190 °C for each reaction to ensure operation in the solvolysis-limited regime, but the temperature of each biomass bed was varied in a range between 160 and 190 °C (Figure 3A). Complete lignin reduction was confirmed by tracking the propyl chain hydrogenation selectivity of the monomers produced. Note that complete hydrogenation of the side

DOI: 10.1021/acssuschemeng.8b01256
ACS Sustainable Chem. Eng. 2018, 6, 7951–7959

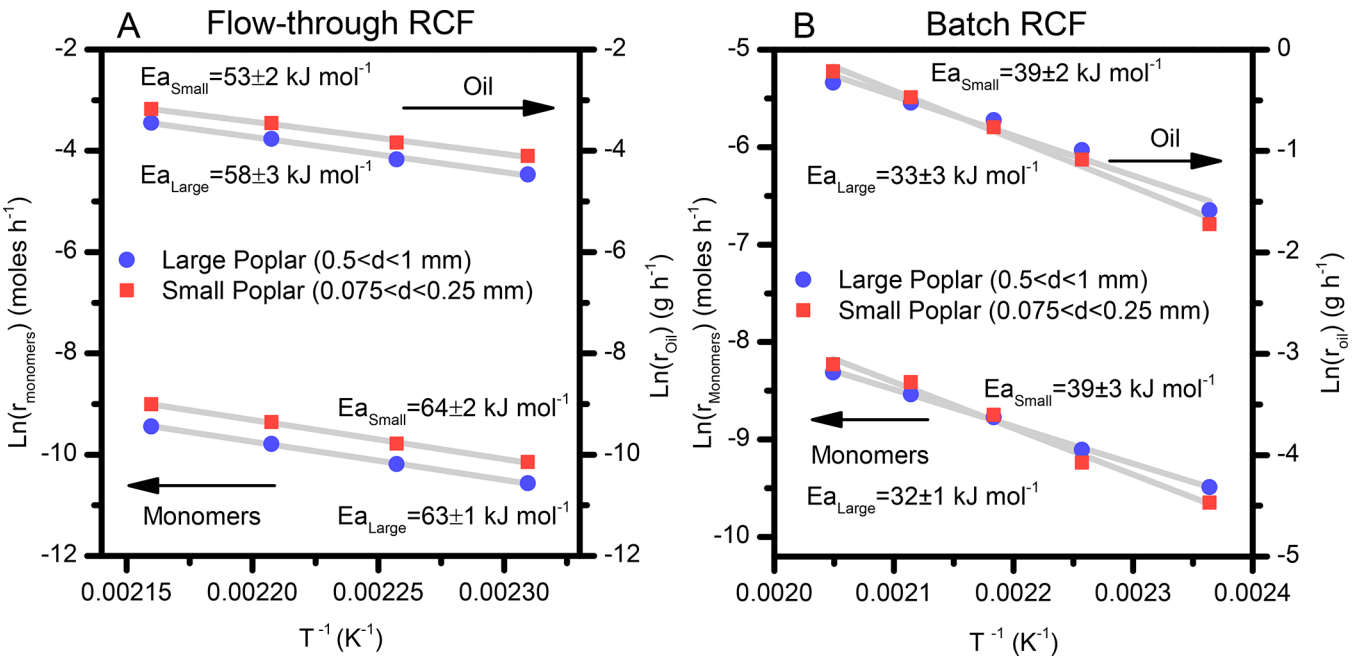

Figure 3. Arrhenius plots for solvolysis-limited RCF reactions performed in (A) flow-through and (B) batch reactors. (A) Apparent activation barriers for flow-through RCF with different size wood particles based on both monomer and lignin oil production rates. (B) Apparent activation barriers for batch RCF with different size wood particles based on both monomer and lignin oil production rates. Batch conditions: milled poplar (1 g, 26% lignin), 15% Ni/C (0.15 g), methanol (50 mL), 30 bar H_2, 150−215 °C, 700 rpm, and 1 h reaction time (0.5−1 h heating ramps). Flow conditions: milled poplar (1 g, 26% lignin), 0.3 g 15% Ni/C (50/50 SiO_2, 100−200 mesh), 50 mL min^{-1} H_2 (60 bar total pressure), 0.5 mL min^{-1} MeOH, 160−190 °C.

chain groups was observed for all experiments performed under solvolysis-limited RCF conditions. Under these conditions, the apparent activation barriers for lignin solvolysis based on monomers and lignin oil were 63 ± 1 and 58 ± 3 kJ mol^{-1}, respectively. These experiments were repeated with smaller biomass particles ($0.075 < d < 0.25$ mm, $Re = 0.08$) resulting in an apparent barriers of 64 ± 2 kJ mol^{-1} for monomers and 53 ± 2 kJ mol^{-1} for lignin oil. The similar activation barriers observed with small and large particle sizes confirm that the solvolysis process is not mass transfer limited in the flow-through reactor, and the similar activation barriers calculated based on monomer and oil yields confirm that the process was operated in the solvolysis limiting regime.

An analogous study performed in batch reactors using the same particle sizes (i.e., $0.5 < d < 1$ and $0.075 < d < 0.25$ mm) at temperatures ranging from 150 to 215 °C and 1 h reaction times with a stirring rate of 700 rpm (Figure 3B) indicated that RCF performed in this reactor configuration is prone to mass transfer limitations. Specifically, batch experiments with the large and small poplar particle sizes generated apparent activation barriers of 32 ± 1 and 39 ± 3 kJ mol^{-1}, respectively. Apparent activation barriers based on total lignin extraction mirrored those based on monomer yields for both wood particle sizes. The low apparent activation barrier observed in the batch system using large particles coupled with the slight increase in the apparent activation barrier when smaller particles were used suggest that the rate of lignin solvolysis in the batch reactor was limited by mass transport.

Diffusion−Reaction Model to Determine Expected Scaling of Mass-Transfer Limitations. The observed scaling in the apparent activation barrier due to mass transfer limitations during the solvolytic extraction of lignin can be predicted by a coupled reaction-diffusion model. Lignin solvolysis requires the diffusion of MeOH into the plant cell wall, where it either liberates lignin polymers from a noncovalent matrix or cleaves lignin-hemicellulose linkages, releasing lignin oligomer fragments.[37,38] Next, these lignin fragments need to diffuse through a tortuous path out of the cell wall and then the wood particle before being transported onto the surface of the redox catalyst. To examine how the differences in flow profiles and lignin fragment concentrations between the two reactor configurations impact the observed activation barriers, we built a one-dimensional reaction-diffusion model depicted in Figure S3. The model defines solvolytic lignin extraction as an equilibrium-mediated reaction on the internal surface of a biomass pore. The concentration of solvent was assumed to be constant throughout the system. The solvent was therefore treated as a constant within the rate expression. By assuming concentration-driven diffusion of lignin fragments inside the pore and an external boundary layer created by convective mass transfer outside of the biomass particle, the lignin fragment concentration profile can be determined analytically.

A shell balance performed in the pore was used to relate the internal diffusion to the surface reaction as shown in eq 1. The Thiele modulus (ϕ), which arises from the nondimensionalization of the equation, is a measure of the ratio of the lignin solvolysis rate to the rate of internal transport. In turn, the Biot number (Bi) measures the proportion of external mass transfer relative to internal mass transfer. The boundary conditions were defined such that there was no diffusion through the walls of the pore and the flux through the external boundary layer must equal the flux of lignin out of the pore opening. The lignin fragment concentration profile can be obtained using eq 2 (see the Supporting Information for the full derivation). An effectiveness factor (η), which is a measure of the apparent

DOI: 10.1021/acssuschemeng.8b01256
ACS Sustainable Chem. Eng. 2018, 6, 7951−7959

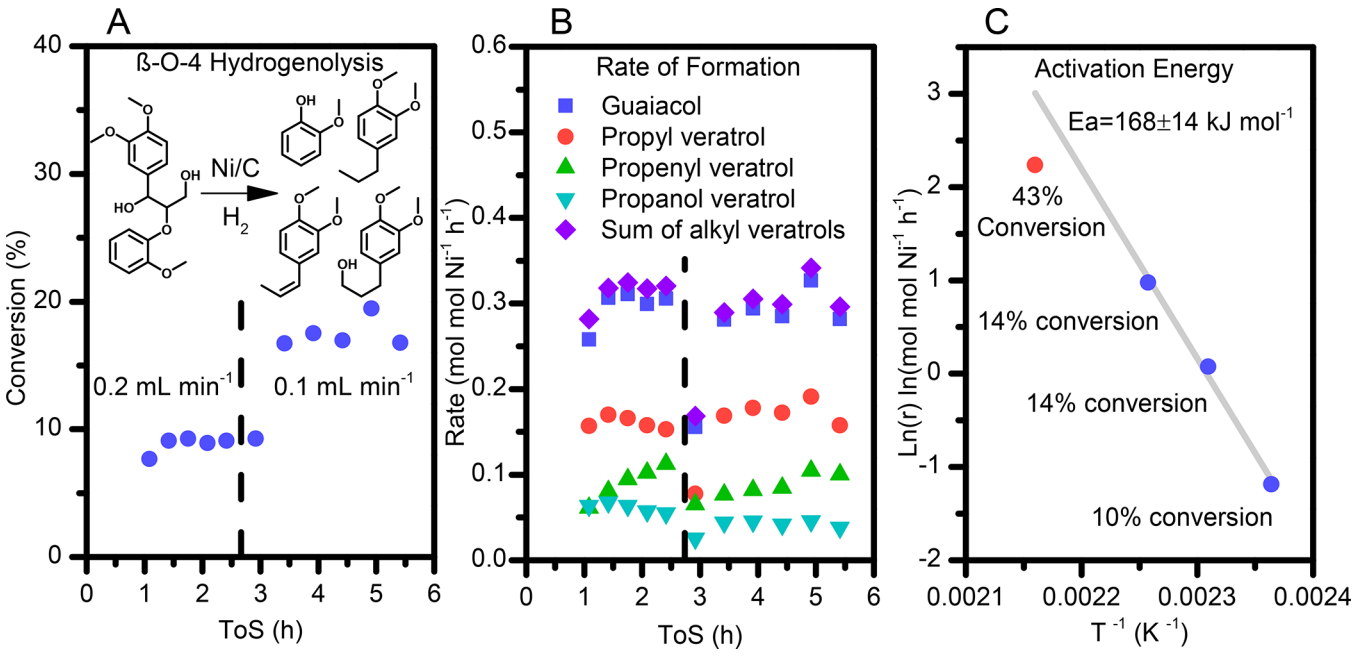

Figure 4. Hydrogenolysis of POPV, a model β-O-4 compound. (A) Reaction scheme and product distribution with reaction conversion time profiles at 150 °C. (B) Production rates of the different products generated at 150 °C. (C) Arrhenius plot for the hydrogenolysis of β-O-4 bonds. Reaction conditions: 0.05 g 5% Ni/C (50/50 SiO_2, 100−200 mesh), 50 mL min^{-1} H_2 (60 bar total pressure). Reactions were performed at 150 °C (0.2 and 0.1 mL min^{-1}, 2 mg mL^{-1} β-0−4), 160 °C (0.4 mL min^{-1}, 2 mg mL^{-1} β-0−4), 170 °C (0.5 mL min^{-1}, 4 mg mL^{-1} β-0−4), and 190 °C (0.6 mL min^{-1}, 4 mg mL^{-1} β-0−4).

observed reaction rate relative to the maximum reaction rate, is a dimensionless metric to understand how mass transfer impacts the observed rate of lignin solvolysis. The maximum reaction rate occurs when there is no mass transfer and the lignin fragment concentration is zero throughout the pore. The observed rate must be equal to the steady state flux of lignin out of the pore as calculated by the model (eq 3). Under severe internal mass transfer limitations, Bi is much larger than ϕ which simplifies η and reveals that the observed reaction rate scales as $(k_L)^{1/2}$ (eq 4). Therefore, when plotting the observed rate in an Arrhenius plot, it is evident that the apparent activation barrier must scale as half of the true kinetic barrier, in agreement with the barriers obtained experimentally when using the kinetically limited flow-through system and the transport-limited batch system. Indeed, when the particle size was reduced in the batch reactor, internal mass transfer was accelerated, leading to an increase in the apparent barrier to 39 kJ mol^{-1}. This effect is expected because the decrease in particle size brings the Bi number closer to ϕ, in which case the full expression for η must be considered. Ultimately, the differences in the reactor configurations and flow profiles manifest as different bulk lignin concentrations and boundary layer thicknesses.

$$\frac{d^2\psi}{d\chi^2} + \phi^2(M-\psi) = 0,\ \left.\frac{d\psi}{d\chi}\right|_{\chi=0} = 0,\ \left.\frac{d\psi}{d\chi}\right|_{\chi=1} = Bi(\gamma - \psi|_{\chi=1})$$

$$\phi = L\sqrt{\frac{2k_L}{DR_p}},\ Bi = \frac{k_m L}{D},\ \gamma = \frac{C_\infty}{C_L},\ \psi = \frac{C}{C_L},\ \chi = \frac{x}{L} \quad (1)$$

$$\psi = M + \frac{Bi(\gamma - M)}{2\phi\sinh(\phi) - 2Bi\cdot\cosh(\phi)}\cosh(\phi\chi) \quad (2)$$

$$\eta = \frac{r_{obs}}{r_{max}} = \frac{\text{area}^*D\left.\frac{d\psi}{d\chi}\right|_{\chi=1}}{\text{area}^*k_L M C_L} = \frac{1}{\phi M}\frac{Bi(\gamma - M)\sinh(\phi)}{\phi\sinh(\phi) - Bi\cdot\cosh(\phi)} \quad (3)$$

$$r_{obs} = \eta 2\pi R_p L r_{max} = \frac{(M-\gamma)}{\phi M}2\pi R_p L k_L M C_L = (M-\gamma)\pi R_p\sqrt{2Dk_L R_p}\,C_L \quad (4)$$

Model Compound Studies to Determine Reduction Limited Activation Barrier. Lignin reduction rates were measured with a model β-O-4 compound (POPV) containing both α and γ hydroxyl groups that are characteristic features of lignin. The reduction was performed by flowing POPV (dissolved in methanol) at a constant flow rate through a packed bed reactor containing 5% Ni/C catalyst. A constant hydrogen stream of 50 mL min^{-1} (STP) was bubbled in shortly before the entrance to the reactor. Four primary products were observed, namely, guaiacol, propyl veratrol, propenyl veratrol, and propanol veratrol, which have identical side chain functionalities to those produced from RCF of whole biomass (Figure 4A). Figure S4−S5 depicts plausible hydrogenolysis, hydrogenation, and hydrodeoxygenation pathways to produce the observed product distribution. Initially, we surmise that the β-O-4 bond is cleaved producing guaiacol and propenol veratrol (not observed), which is then either deoxygenated to propenyl veratrol or hydrogenated to propanol veratrol. These compounds can undergo hydrogenation or hydrodeoxygenation reactions to form propyl veratrol. The differential

DOI: 10.1021/acssuschemeng.8b01256
ACS Sustainable Chem. Eng. 2018, 6, 7951−7959

conversion at 0.2 mL min^{-1} of a 2 mg mL^{-1} solution remained steady at 9% and increased to 17% conversion when the flow rate was decreased by 50% (Figure 4A). The corresponding product distribution and molar rate of formation of each observed product are displayed in Figure 4B. The molar rate of formation of guaiacol and the sum of the alkyl veratrol species (propyl, propenyl, and propanol veratrol) was nearly identical throughout the reaction, indicating that all major products were generated from the cleavage of the β-O-4 bond. Additionally, the molar rate of guaiacol production did not change significantly when the flow rate was decreased, indicating that the reaction was likely not mass transfer limited.

While the overall conversion remained nearly constant over the course of the study, two main factors influenced the product selectivity: catalyst hydrogenation activity and contact time with the catalyst bed. Catalyst deactivation led to a decrease in the propyl veratrol production rate from 0.17 to 0.15 h^{-1} at longer times, and a concomitant increase in the propenyl veratrol production rate from 0.06 to 0.11 h^{-1}. Loss in hydrogenation selectivity over time on a Ni/C catalyst has previously been observed with poplar in flow-through RCF.[31] This model compound study indicated that Ni/C is inherently unstable under RCF conditions. The dependence of selectivity on contact time can be observed in response to reducing the flow rate by 50%, wherein the propyl guaiacol rate increased to 0.18 h^{-1} due to greater hydrogenation and hydrodeoxygenation of propenyl veratrol and propanol veratrol, respectively. An apparent hydrogenolysis activation energy of 168 ± 14 kJ mol^{-1} was measured with a rate of guaiacol production at 150, 160, 170, and 190 °C of 0.3, 1.1, 2.7, and 9.4 mol guaiacol mol Ni^{-1} h^{-1}, respectively (Figure 4C). Similar activation barriers of 149 and 151 kJ mol^{-1} were measured for the acid-catalyzed hydrolysis of POPV and a 4-propylguaiacol analog, respectively.[39] Additionally, the low temperature $T < 120$ °C hydrogenolysis of other model β-O-4 compounds in water had reported activation barriers of 50 kJ mol^{-1} for Pd with a $NaBH_4$ reductant[40] and 86 kJ mol^{-1} for Ni with H_2 gas.[41] The lower barrier obtained in the presence of water may imply a difference in the hydrogenolysis mechanism.

DISCUSSION AND CONCLUSIONS

In this study we isolated the limiting regimes for lignin solvolysis and reduction in RCF of poplar. Using flow-through reactors, intrinsic kinetic parameters were measured for the first time for these two steps by manipulating temperature, catalyst loading, and total hydrogen pressure. Given that these steps are independent from each other, the step with the highest activation barrier may not be the limiting step in the overall process, which is the case for solvolysis limited RCF. Lignin reduction has a high activation energy (168 kJ mol^{-1}) when compared to solvolysis (64 kJ mol^{-1}), but model compound reactions show a much higher monomer production rate than those performed with real biomass. Additionally, the low kinetic activation barrier of lignin solvolysis implies that β-O-4 ethers are not cleaved in this step. The lignin solvolysis rate, however, is limited by the structure of the plant and the nature of the solvent. Therefore, the reduction process does not limit the RCF of biomass under typical conditions reported in literature. Understanding which step is limiting is important when studying different catalysts for RCF, since lignin reduction must be kinetically limiting to accurately compare the activity of different catalysts.

Importantly, RCF studied in both flow-through and batch reactors revealed that under typical RCF conditions the two reactor designs produced different activation barriers for the solvolysis step of RCF. The apparent activation barrier measured in the batch system was half (32 kJ mol^{-1}) of that measured in flow (64 kJ mol^{-1}) implying mass transfer limitations in the batch reactor when operated at conditions typically reported in the literature. This result emphasizes two important differences regarding lignin extraction efficiency and solids mixing between the two reactor types. In flow-through reactors, fresh solvent continuously contacts the biomass bed during extraction, granting the maximum diffusive flux. In contrast, in batch systems the bulk lignin concentration increases as a function of time, progressively decreasing the diffusive flux. Additionally, the mixing within batch vessels is defined by many factors, including the stir rate, biomass particle size, agitator design, and reactor geometry, meaning that the flow properties and transport limitations need to be determined for each batch reactor independently. Conversely, mass transport in flow-through reactors depends solely on the solvent flow rate and the biomass particle size, parameters easily transferable to reactors of different sizes. Regardless of reactor design, our study clearly shows that when performing kinetic measurements on RCF systems, it is important to use the smallest biomass particle size available and consistently check the system for mass transport limitations.

Our results indicating that lignin solvolysis is typically limiting under traditional RCF conditions suggest that future studies for improving the overall RCF process need to focus on improving solvolysis kinetics. This could be accomplished by the use of different solvent pairs or cocatalysts. In this context, it is important to understand how the plant cell wall architecture (which varies both within intra and interspecies) can affect the lignin solvolysis rates, and our approach offers unique opportunities to interrogate different biomass types. In terms of the broader applicability of the kinetic parameters determined in this study, the kinetics of hydrogenolysis should be general for monomer production from biomass since β-O-4 linkages are the most prevalent bonds in lignin regardless of biomass type. The kinetics measured for lignin solvolysis, however, are unique to poplar and methanol because the sugar-lignin linkages and compartmentalization of lignin can be different between different biomass substrates. Therefore, the kinetic parameters of lignin solvolysis must be determined for different substrates, solvents, and cocatalysts. The FDBR is an effective tool for measuring these parameters and will likely play an important role in determining lignin solvolysis rates and benchmarking new RCF systems.

ASSOCIATED CONTENT

Supporting Information

The Supporting Information is available free of charge on the ACS Publications website at DOI: 10.1021/acssuschemeng.8b01256.

Additional figures and tables referenced in the above text (PDF)

AUTHOR INFORMATION

Corresponding Authors

*E-mail: yroman@mit.edu (Y.R.-L.).
*E-mail: gregg.beckham@nrel.gov (G.T.B.).

DOI: 10.1021/acssuschemeng.8b01256
ACS Sustainable Chem. Eng. 2018, 6, 7951−7959

ORCID

Max J. Hülsey: 0000-0002-9894-0492
Gregg T. Beckham: 0000-0002-3480-212X
Yuriy Román-Leshkov: 0000-0002-0025-4233

Notes

The authors declare no competing financial interest.

■ ACKNOWLEDGMENTS

The work was supported by the National Science Foundation, CBET Award No 1454299. Additionally, G.T.B. thanks the US Department of Energy Bioenergy Technologies Office for funding under Contract DE-AC36-08GO28308 with the National Renewable Energy Laboratory. The U.S. Government retains and the publisher, by accepting the article for publication, acknowledges that the U.S. Government retains a nonexclusive, paid up, irrevocable, worldwide license to publish or reproduce the published form of this work, or allow others to do so, for U.S. Government purposes.

■ REFERENCES

(1) Mosier, N.; Wyman, C.; Dale, B.; Elander, R.; Lee, Y.; Holtzapple, M.; Ladisch, M. Features of promising technologies for pretreatment of lignocellulosic biomass. *Bioresour. Technol.* **2005**, *96* (6), 673−686.

(2) Constant, S.; Wienk, H. L. J.; Frissen, A. E.; Peinder, P. d.; Boelens, R.; van Es, D. S.; Grisel, R. J. H.; Weckhuysen, B. M.; Huijgen, W. J. J.; Gosselink, R. J. A.; Bruijnincx, P. C. A. New insights into the structure and composition of technical lignins: a comparative characterisation study. *Green Chem.* **2016**, *18* (9), 2651−2665.

(3) Zakzeski, J.; Bruijnincx, P. C. A.; Jongerius, A. L.; Weckhuysen, B. M. The Catalytic Valorization of Lignin for the Production of Renewable Chemicals. *Chem. Rev.* **2010**, *110* (6), 3552−3599.

(4) Holladay, J. E.; White, J. F.; Bozell, J. J.; Johnson, D. *Top Value-Added Chemicals from Biomass−Volume II—Results of Screening for Potential Candidates from Biorefinery Lignin*, PNNL-16983.

(5) Rinaldi, R.; Jastrzebski, R.; Clough, M. T.; Ralph, J.; Kennema, M.; Bruijnincx, P. C.; Weckhuysen, B. M. Paving the Way for Lignin Valorisation: Recent Advances in Bioengineering, Biorefining and Catalysis. *Angew. Chem., Int. Ed.* **2016**, *55* (29), 8164−8215.

(6) Schutyser, W.; Renders, T.; Van den Bossche, G.; Van den Bosch, S.; Koelewijn, S.-F.; Ennaert, T.; Sels, B. F., Catalysis in Lignocellulosic Biorefineries: The Case of Lignin Conversion. In *Nanotechnology in Catalysis*; Wiley-VCH Verlag GmbH & Co. KGaA, 2017; pp 537−584.

(7) Sun, Z.; Fridrich, B.; de Santi, A.; Elangovan, S.; Barta, K. Bright Side of Lignin Depolymerization: Toward New Platform Chemicals. *Chem. Rev.* **2018**, *118* (2), 614−678.

(8) Deuss, P. J.; Scott, M.; Tran, F.; Westwood, N. J.; de Vries, J. G.; Barta, K. Aromatic Monomers by in Situ Conversion of Reactive Intermediates in the Acid-Catalyzed Depolymerization of Lignin. *J. Am. Chem. Soc.* **2015**, *137* (23), 7456−7467.

(9) Shuai, L.; Amiri, M. T.; Questell-Santiago, Y. M.; Héroguel, F.; Li, Y.; Kim, H.; Meilan, R.; Chapple, C.; Ralph, J.; Luterbacher, J. S. Formaldehyde stabilization facilitates lignin monomer production during biomass depolymerization. *Science* **2016**, *354* (6310), 329−333.

(10) Renders, T.; Van den Bosch, S.; Koelewijn, S. F.; Schutyser, W.; Sels, B. F. Lignin-first biomass fractionation: the advent of active stabilisation strategies. *Energy Environ. Sci.* **2017**, *10*, 1551.

(11) Pepper, J. M.; Lee, Y. W. Lignin and related compounds. I. A comparative study of catalysts for lignin hydrogenolysis. *Can. J. Chem.* **1969**, *47* (5), 723−727.

(12) Yan, N.; Zhao, C.; Dyson, P. J.; Wang, C.; Liu, L.-t.; Kou, Y. Selective Degradation of Wood Lignin over Noble-Metal Catalysts in a Two-Step Process. *ChemSusChem* **2008**, *1* (7), 626−629.

(13) Parsell, T. H.; Owen, B. C.; Klein, I.; Jarrell, T. M.; Marcum, C. L.; Haupert, L. J.; Amundson, L. M.; Kenttamaa, H. I.; Ribeiro, F.; Miller, J. T.; Abu-Omar, M. M. Cleavage and hydrodeoxygenation (HDO) of C-O bonds relevant to lignin conversion using Pd/Zn synergistic catalysis. *Chem. Sci.* **2013**, *4* (2), 806−813.

(14) Song, Q.; Wang, F.; Cai, J.; Wang, Y.; Zhang, J.; Yu, W.; Xu, J. Lignin depolymerization (LDP) in alcohol over nickel-based catalysts via a fragmentation-hydrogenolysis process. *Energy Environ. Sci.* **2013**, *6* (3), 994−1007.

(15) Ferrini, P.; Rinaldi, R. Catalytic Biorefining of Plant Biomass to Non-Pyrolytic Lignin Bio-Oil and Carbohydrates through Hydrogen Transfer Reactions. *Angew. Chem., Int. Ed.* **2014**, *53* (33), 8634−8639.

(16) Galkin, M. V.; Sawadjoon, S.; Rohde, V.; Dawange, M.; Samec, J. S. M. Mild Heterogeneous Palladium-Catalyzed Cleavage of β-O-4′-Ether Linkages of Lignin Model Compounds and Native Lignin in Air. *ChemCatChem* **2014**, *6* (1), 179−184.

(17) Van den Bosch, S.; Schutyser, W.; Vanholme, R.; Driessen, T.; Koelewijn, S. F.; Renders, T.; De Meester, B.; Huijgen, W. J. J.; Dehaen, W.; Courtin, C. M.; Lagrain, B.; Boerjan, W.; Sels, B. F. Reductive lignocellulose fractionation into soluble lignin-derived phenolic monomers and dimers and processable carbohydrate pulps. *Energy Environ. Sci.* **2015**, *8* (6), 1748−1763.

(18) Li, C.; Zheng, M.; Wang, A.; Zhang, T. One-pot catalytic hydrocracking of raw woody biomass into chemicals over supported carbide catalysts: simultaneous conversion of cellulose, hemicellulose and lignin. *Energy Environ. Sci.* **2012**, *5* (4), 6383−6390.

(19) Renders, T.; Schutyser, W.; Van den Bosch, S.; Koelewijn, S.-F.; Vangeel, T.; Courtin, C. M.; Sels, B. F. Influence of Acidic (H3PO4) and Alkaline (NaOH) Additives on the Catalytic Reductive Fractionation of Lignocellulose. *ACS Catal.* **2016**, *6* (3), 2055−2066.

(20) Ferrini, P.; Rezende, C. A.; Rinaldi, R. Catalytic Upstream Biorefining through Hydrogen Transfer Reactions: Understanding the Process from the Pulp Perspective. *ChemSusChem* **2016**, *9* (22), 3171−3180.

(21) Parsell, T.; Yohe, S.; Degenstein, J.; Jarrell, T.; Klein, I.; Gencer, E.; Hewetson, B.; Hurt, M.; Kim, J. I.; Choudhari, H.; et al. A synergistic biorefinery based on catalytic conversion of lignin prior to cellulose starting from lignocellulosic biomass. *Green Chem.* **2015**, *17* (3), 1492−1499.

(22) Van den Bosch, S.; Schutyser, W.; Koelewijn, S. F.; Renders, T.; Courtin, C. M.; Sels, B. F. Tuning the lignin oil OH-content with Ru and Pd catalysts during lignin hydrogenolysis on birch wood. *Chem. Commun.* **2015**, *51* (67), 13158−13161.

(23) Anderson, E. M.; Katahira, R.; Reed, M.; Resch, M. G.; Karp, E. M.; Beckham, G. T.; Román-Leshkov, Y. Reductive Catalytic Fractionation of Corn Stover Lignin. *ACS Sustainable Chem. Eng.* **2016**, *4* (12), 6940−6950.

(24) Jastrzebski, R.; Constant, S.; Lancefield, C. S.; Westwood, N. J.; Weckhuysen, B. M.; Bruijnincx, P. C. Tandem Catalytic Depolymerization of Lignin by Water-Tolerant Lewis Acids and Rhodium Complexes. *ChemSusChem* **2016**, *9* (16), 2074−2079.

(25) Huang, X.; Zhu, J.; Korányi, T. I.; Boot, M. D.; Hensen, E. J. Effective Release of Lignin Fragments from Lignocellulose by Lewis Acid Metal Triflates in the Lignin-First Approach. *ChemSusChem* **2016**, *9* (23), 3262−3267.

(26) Huang, X.; Gonzalez, O. M. M.; Zhu, J.; Korányi, T. I.; Boot, M. D.; Hensen, E. J. Reductive fractionation of woody biomass into lignin monomers and cellulose by tandem metal triflate and Pd/C catalysis. *Green Chem.* **2017**, *19* (1), 175−187.

(27) Schutyser, W.; Van den Bosch, S.; Renders, T.; De Boe, T.; Koelewijn, S. F.; Dewaele, A.; Ennaert, T.; Verkinderen, O.; Goderis, B.; Courtin, C. M.; Sels, B. F. Influence of bio-based solvents on the catalytic reductive fractionation of birch wood. *Green Chem.* **2015**, *17* (11), 5035−5045.

(28) Huang, X.; Zhu, J.; Korányi, T. I.; Boot, M. D.; Hensen, E. J. M. Effective Release of Lignin Fragments from Lignocellulose by Lewis Acid Metal Triflates in the Lignin-First Approach. *ChemSusChem* **2016**, *9* (23), 3262−3267.

(29) Van den Bosch, S.; Renders, T.; Kennis, S.; Koelewijn, S. F.; Van den Bossche, G.; Vangeel, T.; Deneyer, A.; Depuydt, D.; Courtin, C. M.; Thevelein, J. M.; Schutyser, W.; Sels, B. F. Integrating lignin valorization and bio-ethanol production: on the role of Ni-Al2O3

DOI: 10.1021/acssuschemeng.8b01256
ACS Sustainable Chem. Eng. 2018, 6, 7951−7959

catalyst pellets during lignin-first fractionation. *Green Chem.* **2017**, *19* (14), 3313−3326.
(30) Luo, H.; Klein, I. M.; Jiang, Y.; Zhu, H.; Liu, B.; Kenttämaa, H. I.; Abu-Omar, M. M. Total Utilization of Miscanthus Biomass, Lignin and Carbohydrates, Using Earth Abundant Nickel Catalyst. *ACS Sustainable Chem. Eng.* **2016**, *4* (4), 2316−2322.
(31) Anderson, E. M.; Stone, M. L.; Katahira, R.; Reed, M.; Beckham, G. T.; Román-Leshkov, Y. Flowthrough Reductive Catalytic Fractionation of Biomass. *Joule* **2017**, *1* (3), 613−622.
(32) Kumaniaev, I.; Subbotina, E.; Savmarker, J.; Larhed, M.; Galkin, M. V.; Samec, J. S. M. Lignin depolymerization to monophenolic compounds in a flow-through system. *Green Chem.* **2017**, *19* (24), 5767−5771.
(33) Sergeev, A. G.; Hartwig, J. F. Selective, Nickel-Catalyzed Hydrogenolysis of Aryl Ethers. *Science* **2011**, *332* (6028), 439−443.
(34) Sluiter, A.; Sluiter, J.; Templeton, D.; et al. *Determination of Extractives in Biomass*, Technical Report NREL/TP-510-42619; 2005.
(35) Sluiter, A.; Hames, B.; Ruiz, R.; Scarlata, C.; Sluiter, J.; Templeton, D.; Crocker, D. *Determination of Structural Carbohydrates and Lignin in Biomass*, Technical Report NREL/TP-510-42618; 2008.
(36) Dwivedi, P. N.; Upadhyay, S. Particle-fluid mass transfer in fixed and fluidized beds. *Ind. Eng. Chem. Process Des. Dev.* **1977**, *16* (2), 157−165.
(37) Gierlinger, N.; Schwanninger, M. Chemical Imaging of Poplar Wood Cell Walls by Confocal Raman Microscopy. *Plant Physiol.* **2006**, *140* (4), 1246−1254.
(38) Donaldson, L. A.; Knox, J. P. Localization of Cell Wall Polysaccharides in Normal and Compression Wood of Radiata Pine: Relationships with Lignification and Microfibril Orientation. *Plant Physiol.* **2012**, *158* (2), 642−653.
(39) Sarkanen, K. V.; Hoo, L. H. Kinetics of Hydrolysis of Erythro-Guaiacylglycerol β-(2-Methoxyphenyl) Ether and Its Veratryl Analogue Using Hc1 and Aluminum Chloride As Catalysts. *J. Wood Chem. Technol.* **1981**, *1* (1), 11−27.
(40) Galkin, M. V.; Dahlstrand, C.; Samec, J. S. M. Mild and Robust Redox-Neutral Pd/C-Catalyzed Lignol β-O-4′ Bond Cleavage Through a Low-Energy-Barrier Pathway. *ChemSusChem* **2015**, *8* (13), 2187−2192.
(41) He, J.; Zhao, C.; Lercher, J. A. Ni-Catalyzed Cleavage of Aryl Ethers in the Aqueous Phase. *J. Am. Chem. Soc.* **2012**, *134* (51), 20768−20775.

DOI: 10.1021/acssuschemeng.8b01256
ACS Sustainable Chem. Eng. 2018, 6, 7951−7959